Available online at www.sciencedirect.com

SciVerse ScienceDirect

Ceramics International 39 (2013) 6533–6542

CERAMICS INTERNATIONAL

www.elsevier.com/locate/ceramint

Micro-porous calcium phosphate coatings on load-bearing zirconia substrate: Processing, property and application

Jing-Zhou Yang[a,b], Rumana Sultana[a], Paul Ichim[c], Xiao-Zhi Hu[a,*], Zhao-Hui Huang[b], Wei Yi[a], Bin Jiang[a], Youguo Xu[b]

[a]School of Mechanical and Chemical Engineering, University of Western Australia, Perth, WA 6009, Australia
[b]School of Materials Science and Technology, China University of Geosciences (Beijing), Beijing 100083, PR China
[c]School of Dentistry, University of Western Australia, Perth, WA 6009, Australia

Received 7 October 2012; received in revised form 25 January 2013; accepted 25 January 2013
Available online 8 February 2013

Abstract

This study presents the design, processing, properties and potential applications of a novel layered bio-ceramic composites consisting of three different micro-porous calcium phosphate coatings on strong zirconia cores manufactured using a recently developed slip coating-deposition and coating-substrate co-sintering technique. Detailed microstructures of the three graded micro-porous calcium phosphate coatings, and the coating/substrate interface have been investigated. Also, the flexural strength of the bio-ceramic composite and the bonding state between the coatings and zirconia substrate have been characterized. A preliminary and limited in vitro cell test indicates that the new scaffold composite has no cytotoxicity to the fibroblasts which can attach, proliferate and grow on the coating surfaces. Because of the combination of bio-function and strength, such layered load-bearing bio-ceramic composites are a potential candidate for large-scale head bone repairs.

Keywords: A. Sintering; B. Microstructure; C. Strength; E. Biomedical application; Apatite-zirconia composite

1. Introduction

The intended use of artificial bio-functional bone scaffolds is for implantation in critical size hard tissue defects which in some cases need to sustain mechanical loading [1]. The ceramic scaffolds have drawn significant interest in the past years and experimental data shows that hydroxyapatite/tri-calcium phosphate (HA/TCP) scaffolds structures with open pores larger than 100 μm are bio-resorbable and osteoconductive [2–5]. However, such scaffolds can be used as implants/spacers mostly for small bone defect and light-load-bearing bone defect repairs, because of their inadequate mechanical performance, with a compressive strength in the range of 2–36 MPa [6]. Even the fully dense hydroxyapatite ceramic only exhibits a bending strength of 100 MPa.

A load bearing device provides mechanical stability at the time of implantation and, by gradually transferring the load to the bone, stimulates bone healing [1]. Significant efforts have been made to build load bearing scaffolds. Cesarano et al. [7] used a robocasting technique to produce a load bearing HA lattice scaffold with hierarchical porosity and the compressive strength similar to the cortical bone. Using double slip-casting method, Zhang et al. manufactured a strong HA scaffold with a bending strength of 73.3 MPa [8].

Because the bending strength of compact bones ranges from 50 MPa to 300 MPa [9] the immediate or heavy load-bearing capacity of calcium phosphate based scaffolds for large scale bone defects such as cranioplasty or mandibular recosntructions is obviously limited.

In addition to carrying the motion generated by muscle contractions, some clinical applications of rigid scaffolds require for these to provide physical protection of the organs they cover, as is the case of titanium plates (Fig. 1a) and scaffold-like meshes [10,11] used for cranioplasty defect repair as it is essential to preserve the brain safety.

*Corresponding author. Tel.: +61 8 6488 2812; fax: +61 8 6488 1024.
E-mail addresses: xhu@mech.uwa.edu.au, xiao.zhi.hu@uwa.edu.au (X.-Z. Hu).

0272-8842/$ - see front matter © 2013 Elsevier Ltd and Techna Group S.r.l. All rights reserved.
http://dx.doi.org/10.1016/j.ceramint.2013.01.086

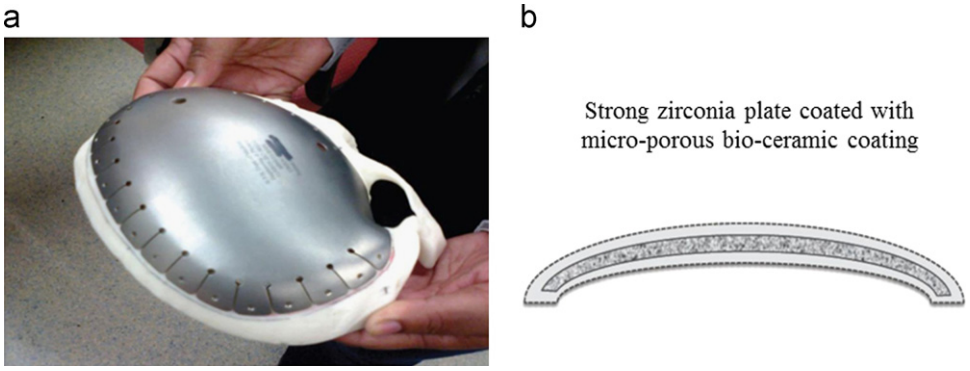

Fig. 1. (a) Commercial cranioplasty titanium plate used in Royal Perth Hospital [12]; (b) sketch of thick bio-ceramic coated zirconia based plate.

For such mechanical demanding environments, titanium is the current material of choice. For example, there are 15 commercial titanium cranioplasty custom plates available for clinic applications at Royal Perth Hospital in Western Australia [12].

The mechanical properties of titanium based metal implants are excellent, well documented and adequate for load bearing large scale bone replacement. The major shortcoming however, is the bio-inert behavior of titanium that lacks osteoconduction. A common method to improve the biological integration of an otherwise bio-inert material is to cover it with a bio-active coating. Various coating techniques and materials have been described [13–16] and amongst which calcium phosphate coated stem surfaces have shown excellent bone on-growth [17]. A common shortcoming of coated metal implants is the thickness and porosity of the coat which is often limited [13,15,16] and as such offers a reduced volumetric anchorage for bone in-growth.

An alternative to coated metal could be to use a strong thin ceramic plate on which a graded scaffold-like porous bio-ceramic coating is build. A sketch of such a composite is shown in Fig. 1b.

The scope of the present work is to study the feasibility of manufacturing a strong layered bio-ceramic composite consisting of a graded porous bio-active calcium phosphate coating bonded on load bearing zirconia substrate using a newly-developed slip coating deposition and coating/substrate co-sintering technique [18]. The hierarchical porous structure of the coating and coating/substrate interface were characterized and preliminary analyses of the bending strength and in vitro biocompatibility were completed to identify the suitability of the proposed composite as an alternative to titanium.

2. Materials and methods

2.1. Raw materials

The main starting materials employed in this study were yttria stabilized zirconia (3Y-TZP) (TZ-3Y E, <200 nm, Tosoh Co., Japan), hydroxyapatite (HA) (<200 nm, Sigma-Aldrich Co., USA), and alumina (α-Al_2O_3) (AKP50, purity $>99.99\%$, <300 nm, Sumitomo, Japan). Besides, dolapix (Aschimmer and Schwarz Gmbh, Germany) was used as dispersant, PVA solution (9 wt%) as binder, and distilled water as solvent. Polymethylmethacrylate (PMMA, Sigma Aldrich, USA) micro-beads (20–50 μm) and cooking potato starch powders with size of 1–20 μm were chosen as pore generators.

2.2. Construction of scaffold-like coating

Zirconia based substrate containing 30 vol% HA was formed through die-pressing and then pre-sintered at 900 °C. One surface of the substrate was covered with three layers (transition, middle and top layer) of coating using slip-coating deposition technique. The processing details required to obtain the substrate and of the deposition technique are presented in detail in our previous study [18]. In brief, green coatings and pre-sintered substrates are dried in wet air for 24 h and in dry air for another 24 h, then finally co-sintered at 1300 °C for 2 h. During its final sintering step, the HA incorporated in the substrate will further decompose to tri-calcium phosphate and generate micro-pores. These micro-pores are required for the coating deposition and its bonding onto substrate. Because the substrate is pre-sintered, it has a good water-absorption ability which will facilitate thicker coating deposition compared with applying slip/slurry coating on the fully sintered ceramic substrate. After the coating process, thermal and intrinsic residual stresses are generated inevitably [19] due to the significant mismatch of thermal expansion coefficient and Young's modulus of the coating and the substrate. These residual stresses may cause cracks and delamination of the interfaces in the scaffold [20,21]. A number of processing procedures are therefore employed to reduce the residual stresses and to obtain a crack free composite material. Firstly, the coating is deposited in a multilayered fashion with graded composition and porosity and it has been shown previously that this technique assist with reduction of residual stresses and achieving a delamination-free substrate/coating interface [18]. Additionally, because HA is added in the substrate and ZrO_2 in

the transition coating layer, TCP can form in the composite thus improving the substrate-coating bonding. To further reduce the mismatch of thermal expansion coefficients between the calcium phosphate coating and ZrO_2 based substrate, alumina is also incorporated in the coatings.

To generate the porosity of the scaffold-like coating we have used PMMA spherical micro-beads. 15 wt%, 15 wt% and 25 wt% starch powders are also added in the transitional layer, middle layer and top layer respectively to improve the overall interconnectivity of the coatings. The distribution of the components to achieve the graded structure is given in Fig. 2 below. The optimal processing procedures employed in the production of final composite have been identified by trial and error.

2.3. Phase composition and microstructure characterization

The phase change of the coating layer after heat treatment was characterized using X-ray diffraction (Siemens D5000 diffractometer, Munich, Germany) using CuKa1 radiation at a scanning rate of 1.2 °/min. The sample used for XRD is bulk composite with coating. For analyzing the coating/substrate interface microstructure, the samples were embedded in the resin (EpoFix epoxy, Struers A/S, DK-2750 Ballerup, Pederstrupvej 84, Denmark) and polished with diamond grinding plates with final size of 1 μm [22]. The resin embedding was necessary to preserve the porous structure during sectioning and polishing. Multiscale porous structures of the coatings and coating/substrate interface were then observed with a field emission scanning electron microscope Zeiss 1555 (Carl Zeiss Inc., Oberkochen, Germany). A focused ion beam miller (Focused Ion Beam xP200, FEI Company, Hillsboro, OR 97124 USA) was also used to obtain views of the inner porous structure of the coatings.

2.4. Mechanical properties characterization

To determine the load-bearing capacity of newly constructed coating-substrate composite we have used a simple bending strength test [23]. For this purpose, a total of six samples (3 mm × 4 mm × 40 mm) were tested in three point bending using with an Instron 4301 (Instron Company, Norwood, MA 02062-2643, USA) testing machine. The crosshead speed was 0.5 mm/min and the jig span was 20 mm. All the coating-substrate composite samples were placed with the substrate facing the loading roll and the coating facing the spanners. For control, we have used six samples identical in size which consisted only of the substrate (ZrO_2 + 30 vol% HA) without the porous coating.

The coating/substrate bonding strength tests were conducted via the method shown in ASTM C633-01. 15 mm × 15 mm × 3 mm square zirconia based ceramic samples with calcium phosphate coatings were used for bonding strength measurements. Two steel rods with diameters of 10 mm were made for connecting the sample and testing machine fixture. "Araldite super strength A & B glue" was used as bonding agent, which can get the maximum strength after 24 h. The steel rods with sample adhering on, as shown in Fig. 2, were pin-fixed into the testing machine. The cross-head speed was 0.1 mm/min. Two tests were carried out on each type of sample with single/double/triple layered coatings. The bonding strength is calculated by maximum load/contact area. In order to check the coating/substrate interfacial bonding condition and the microstructure of the coating, the fracture surface resulting from bonding strength test was observed by scanning electron microscopy.

2.5. In vitro cell test

A preliminary in vitro cell test was also completed to investigate if the porous scaffold-like coating has any cytotoxicity and cells can attach, proliferate and grow on the coating surfaces. This test was employed because there are some other minor phases besides TCP main phase in the coating whose effect in the amount which results from the processing on the cells cannot be predicted.

For this purpose, cytotoxic and cellar response tests were carried out in vitro using the Methyl thiazolyl tetrazoliun (MTT) method [24,25]. A number of rectangular samples were used in this preliminary biocompatibility testing. The cytotoxic and cellular response was compared with controls groups of titanium, high purity alumina ceramic and a blank group. We have used titanium and alumina as controls because they are the materials most commonly used for bone implants [26–31]. All the samples and negative control materials were sterilized in an autoclave at 2 bars, 120 °C for 30 min.

L929 mouse fibroblast cells (Beijing Stomatological Hospital & School of Stomatology, Capital Medical

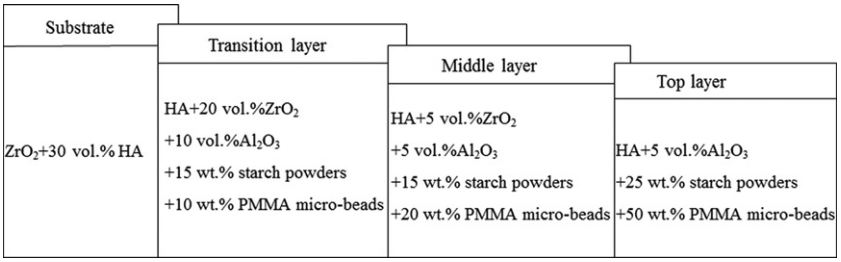

Fig. 2. Diagram showing the distribution of the slurry components for coatings.

University, Beijing, PRC) were cultured in the flasks at 37 °C and 5% CO_2 in an alpha-minimum essential medium (α-MEM). 0.25% Trypsin (Sigma-Aldrich Co. LLC., St. Louis, MO 63178, USA) digests proteins that anchor cells to the tissue culture substrate, thereby detaching them, and $1 \times 10^4\ mL^{-1}$ cell suspension was prepared with 10% bovine serum solution (Hangzhou Sijiqing Biological Engineering Materials Co., Ltd., PRC) and filled into 96-well culture plates (Corning Inc., Corning NY 14831 USA), with each well of 100 μL of suspension. The culture plates were placed in an incubator (5% CO_2+95% air) at 37 °C for 24 h.

The culture medium was changed every two days until the cells reached a confluence of 95%, as determined visually with an inverted microscope. Then the primary medium was removed and the remnant was washed with buffer phosphate solution twice (PBS, Hangzhou Jinuo Biological Medical technology Co., Ltd., PRC). Then 100 μL of the leached liquids from the four groups (TCP based coatings, titanium alloy, high purity alumina ceramic and blank) were added to the culture plates, respectively, with continued culturing in the environment. An inverted phase contrast microscope was used to determine the cellular morphologies after 72 h of the culture. Each well of the culture plates was added with 20 μL MTT (Sigma-Aldrich Co. LLC., St. Louis, MO 63178, USA) liquid with concentration of 5 mg/mL and continued to culture for 4 h, and then the primary medium was removed from the wells. 150 μL dimethyl sulphoxide (DMSO, Chemical Reagent Beijing Co., Ltd., PRC) was added to each well, and the plates were vibrated in an oscillator for 10 min to dissolve completely the remnant. The absorbance at the wave length of 490 nm was a measured on a plate reader. The relative growth rate (RGR) of cells was calculated by the following equation:

$$RGR = (A_t/A_b) \times 100\%$$

where A_t and A_b are the absorbance value for the trial group and blank group, respectively.

After 72 h the cultures were washed with PBS. Cells were fixed with a solution containing 3 vol% glutaraldehyde (Sigma, China) and 3 vol% paraformaldehyde (Sigma, China) in 0.2 M sodium cacodylate buffer (pH 7.4) and rinsed three times with PBS. For cell observation using scanning electron microscopy, all samples were dehydrated in a graded acetone series (10, 30, 50, 75, 90, 95, 98 and 100 vol.%). Samples were maintained at 100 vol.% acetone and super critical-point dried. The samples were coated with gold before observed by a scanning electron microscope (SEM) of Hitachi S4800 (Hitachi High-Tech. Co., Tokyo, Japan) to characterize the morphologies of L929 cells cultured on the coating sample surface.

3. Results

3.1. Microstructure and composition of the scaffold-like coating

An SEM overview of the triple-layered TCP based coating cross-section is shown in Fig. 3a. The coating shows the three layers, with the top layer consisting of TCP, whereas the middle and transition layers have different contents of ZrO_2 and Al_2O_3 (white phase). The main phase in the transition/middle layer is TCP (gray phase).

XRD analysis shows the phase composition of TCP-rich coating. In the sintered top layer the final phases are TCP, TTCP ($Ca_4(PO_4)_2O$), α-Al_2O_3 and $CaAl_4O_7$ (Fig. 4a). By contrast the in the middle layer the phases are TCP, ZrO_2, α-Al_2O_3 and $CaZr_4O_9$ (Fig. 4b). HA can decompose form TCP and TTCP when subjected to temperatures over 1350 °C, as illustrated in (1) below. Some of the TCP and TTCP can be rehydrated to HA when the sintering temperature is lowered below 1100 °C. The detailed phase transformation process is reported elsewhere [32,33]

$$Ca_{10}(PO_4)_6(OH)_2 \rightarrow 2Ca_3(PO_4)_2 + Ca_4(PO_4)_2O + H_2O \quad (1)$$

Because zirconia and alumina can promote the decomposition of HA at the temperature below 1300 °C the process could be described by the following equations:

$$2Ca_{10}(PO_4)_6(OH)_2 + 4ZrO_2 \rightarrow 5Ca_3(PO_4)_2 + Ca_4(PO_4)_2O + CaZr_4O_9 + 2H_2O \quad (2)$$

$$2Ca_{10}(PO_4)_6(OH)_2 + 2Al_2O_3 \rightarrow 5Ca_3(PO_4)_2 + Ca_4(PO_4)_2O + CaAl_4O_7 + 2H_2O \quad (3)$$

In our samples we could not trace HA in the sintered coatings.

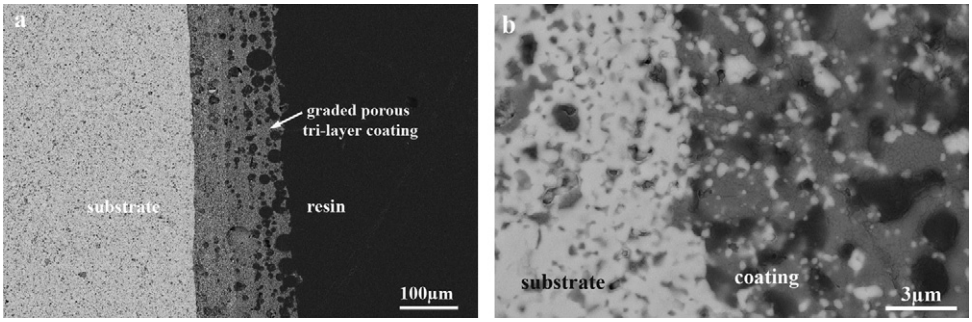

Fig. 3. Cross-sectional surface microstructure of the gradient porous coating on zirconia based substrate: (a) Overview; (b) close-up of the interface.

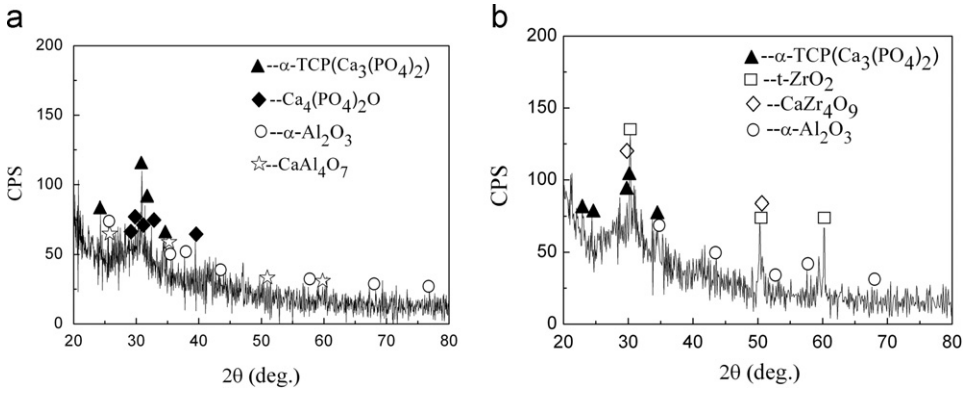

Fig. 4. XRD patterns of the solid coating layers after finally sintering at 1300 °C for 2 h: (a) top layer; (b) middle layer.

It can be seen from Fig. 3 that the resulting scaffold-like coating has an open porous structure with micro pores with the size ranging from 20 to 50 μm. The total thickness of the graded porous tri-layer coating is around 200 μm. Furthermore, the direct observation indicates that the interfacial bonding state between the coating and zirconia substrate is excellent, as no cracks or delamination can be observed along the interface, as shown in Fig. 3b.

SEM observation of the top, middle and transitional layers shows that they are all crack-free and with an open gradient porous architecture (Fig. 5). As it is further shown in Fig. 7 there are some submicro/nano pores in the walls of the bigger spherical open pores, however the level of interconnectivity of the whole porous structure still needs to be increased. The three coating layers have scaffold-like porous structures with the largest spherical pores of about 50 μm diameter. Micro pores smaller than 20 μm can also be observed in the connecting parts and the walls of pores, thus preserving the overall microsieve-like aspect throughout the entire thickness of the porous coating. Considering the size of the pores, the SEM observation indicates that the larger pores result from PMMA micro-beads burn-out whereas the smaller ones mainly derive from starch powders were burned out and HA particles sintering.

3.2. Mechanical testing of coating-substrate composite

The three-point bending test showed that the coating /substrate composite has bending strength of 320 ± 23 MPa. The bending strength of the zirconia based substrate without coating is 390 ± 54 MPa. Table 1 shows the results of the three-point bending testing.

Based on the calculations, the bonding strength averages 24 MPa. During the tensile bonding strength test in the sample with triple/double-layer coating the fracture occurred within the coating which is highly porous and rather weak. Therefore this indicates that the coating/substrate bonding strength is higher that the strength of the porous coating. This is further supported by the results of the bonding strength in single-layer (transitional layer) samples. Here the adhesive separation occurred at the coating/glue interface and a maximum tensile load of 1900 N was obtained.

3.3. In vitro test results for the coating

The cytotoxicity of the coatings was evaluated and relative growth rate (RGR) was calculated after the L929 mouse fibroblast cells growing for 72 h. The RGR values of transitional/middle/top layer coating and control materials are 90, 90, 85 and 93, respectively. It is obvious that the RGR values of the coatings are close to those of negative control materials, which means the cells can proliferate well on the non-cytotoxic calcium phosphate coating. The results further indicate that various compositions and porous structures of the three coating layers have virtually no influence on the cellar response.

The morphologies of the cells cultured on the coating surfaces for 72 h were observed by SEM. Fig. 8 shows the cells attaching on the surfaces of TCP-rich coatings have similar morphologies compared with negative control materials of bio-medical titanium alloy. Elongate compressed mouse fibroblast cells can be found on the coating surface, as displayed in Fig. 8a. As can be seen in Fig. 8b the cells attached to coating surface have lots of fibre-like pseudopodia around the cell bodies.

4. Discussions

The main shortcoming of the existing calcium phosphate ceramics is their limited load-bearing capacity. Load bearing capacity is required for implants used to repair and reconstruct critical size bone defects in bones such as skull, the femur [34,35] or in bones which experience complex deformation during function loading [36,37] such as the mandible. Bone has a hierarchical porous architecture [38], and its bending strength upper limit is about 300 MPa [9]. Calcium phosphate ceramic/cement and biopolymer scaffolds for bone defect reconstruction have been developed and studied in vitro and in vivo in the past decades [3,4,39–42]. HA/TCP scaffolds have good biocompatibility but inadequate mechanical properties and the

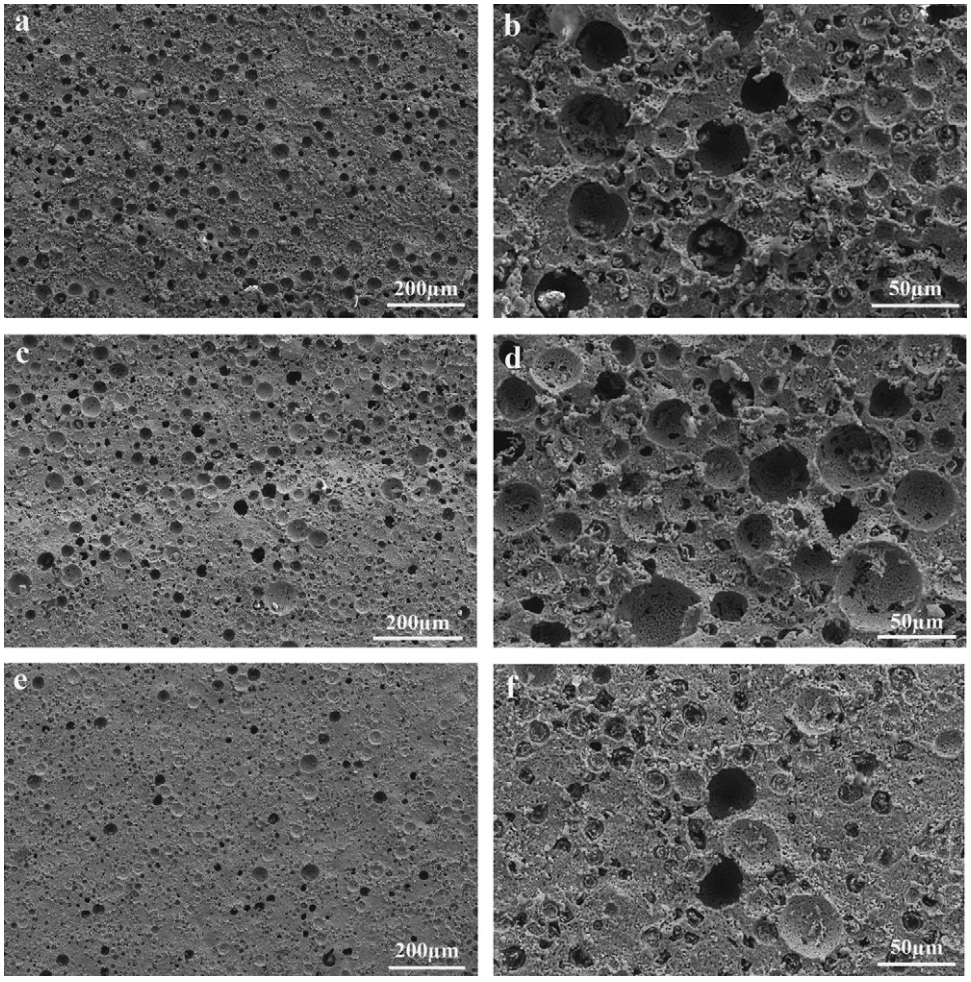

Fig. 5. Sintered surface microstructures of coating layers: (a) overview and (b) detailed porous structure of the top layer; (c) overview and (d) detailed porous structure of the middle layer; (e) overview and (f) detailed porous structure of the transition layer.

Table 1
The bending strengths of coated and uncoated zirconia based substrates.

Samples	Bending strength (MPa)						Average (MPa)	SD (MPa)
	#1	#2	#3	#4	#5	#6		
substrate without coating	319.4	415.8	353	362.6	362	403	390	54
Substrate with coating	337.8	300	321.6	281.3	323.9	351.2	320	23

typical bending strength of such scaffolds is merely few MPa [43,44]. Although a scaffold bone replacement does not have to be as strong as native bone considering that bone fractures most often heal via the formation of cartilaginous template that is subsequently ossified and remodeled and the strength of the implanted scaffold can be augmented, the immediate load-bearing capacity still needs to be enhanced to avoid using an extra strong metal device (must be taken out by the second surgery after the new bone forms) to support and fix the scaffold.

To achieve an increase in the load-bearing capacity of the calcium phosphate scaffold one can strengthen the bulk scaffolds by employing new processing technique [7,8] or alternatively, one can use porous coatings on strong substrates. The latter alternative has been employed in this work to produce load-bearing bone scaffolds. The method is based on our previous work in which we have successfully produced a graded micro porous 40 μm thick calcium phosphate coating on zirconia based substrate using a newly developed low density slip coating-deposition and coating-substrate co-sintering technique.

By employing this method we have successfully fabricated scaffold-like TCP-rich thick coatings with micro and sub-micro/nano porosity on the strong zirconia based substrate. ZrO_2 and Al_2O_3 sub-micro powders were incorporated in the coating to promote the decomposition of HA to form TCP and generate sub-micro/nano pores.

The newly developed coating-substrate composite shows an excellent bending strength, and our limited preliminary data indicates that it exceeds the one of the bone (320 MPa vs 300 MPa) which creates an over-abundant mechanical

reserve for the composite to functionally integrate with the bone. To best of our knowledge, our work is a first in this direction. Previous work of other groups produced scaffolds with improved mechanical properties, such as Cesarano et al. [7] who manufactured an improved bulk scaffold with a compressive strength of 195 MPa but they did not report on the bending strength.

The three-point bending test has shown a decrease in the bending strength of the coating samples, however the resulting bending strength still supersedes that of bone. This modest reduction can be explained by the sensitivity of mechanical testing of ceramics are to machined surface conditions. For the coating-substrate composite, the coated side of the substrate has been roughed with 320# silicon carbide sand paper for achieving a strong mechanical interlocked interface between the coating and the substrate before applying the coating. By contrast, the uncoated zirconia based substrates, the samples were well polished before measuring their bending strength. During the three point bending test all the samples were placed with the substrate facing the loading roll and the coating facing the spanners and as such the surface quality influences the stresses profile in the tension area.

Due to its superior mechanical strength, the present layered ceramic composite may offer an alternative to metal-only implants (such as titanium) used currently to replace critical bone defects [28,45,46]. It was shown by our results that the increase in TCP after sintering has a limited effect on the bending strength. This can be further converted into an additional advantage as one can control the fracturing properties by varying the HA content in the slurry. Therefore, the bending strength of the TCP-containing zirconia based substrate can be tailored by modifying the TCP content. This provides the ability to create site and patient specific tailored implants.

In addition to superior mechanical strength, the present composite has a scaffold-like porous coating with a hierarchical porous structure and enough thickness required for bone ingrowth and colonization. We have shown that the coating has an open porous architecture, which has been shown to have a notable effect on the osteoconductivity and bone ingrowth rate [3–5]. This was also illustrated by Woodard et al. [42] that showed that the hierarchical micro porous structure may be helpful for implant material to increase osteoconductivity required for bone regeneration.

It has been also shown that nano-scale surface features for implant materials are promising to enhance the tissue regeneration capacity [47,48]. The present coating on strong substrate has sub-micro/nano pores which result from the decomposition of HA during sintering process, accompanied by gassy water release.

Because the small amount of ZrO_2 added in the transition/middle layer can promote the decomposition of HA and also react with HA, more sub-micro/nano pores form in the transition/middle layer compared with top layer. Fig. 7c and d show the multi-scale porous structure of the coating across the fracture surface of one of the samples, illustrating the sub-micron and nano-sized pores. The degree of interconnectivity needs to be improved to assist cell migration in enhancing osseointegration and bone regeneration, although the multi-scale porous component interconnects to form micro channels.

In addition of the bending strength and hierarchical porous structure, interfacial bonding condition is also highly concerned and vital for bio-ceramic coated artificial bone implants. The bonding strength test and SEM observations support that the interfacial bonding between the graded porous bio-coating and strong substrate is quite strong. Fig. 3b presents that the coating/substrate interface bonding is good as no delamination or micro cracks along the interface. As shown in Fig. 6, tensile tests were carried out on samples with single/double/triple-layer porous coating to measure the coating/substrate bonding strength. For the sample with triple/double-layer coating, during the tensile test, fracture occurred within the coating which is highly porous and weak. It is suggested that the coating/substrate bonding strength is higher that the strength of the porous coating. For the sample with single-layer (transitional layer) coating, fracture took place along the coating/glue interface and a maximum tensile load of 1900 N was obtained. Based on the calculation the bonding strength is around 24 MPa. The fracture surface derived from bonding strength test for the sample with single-layer coating was observed by SEM to further understand interfacial bonding condition. As shown in Fig. 7a, there was still some coating adhering on the substrate, which indicated that the bonding strength is even higher. It can be concluded the interface bonding between the transitional coating and the zirconia based substrate is quite strong.

The biocompatibility and bioactivity of the present porous calcium phosphate based coatings was assessed by their in vitro cellular responses. The relative growth rate (RGR) values of the coatings are close to those of negative control materials, which indicate the cells can proliferate well on the non-cytotoxic calcium phosphate coating. We also show that various compositions and porous structures of the three coating layers have minimal, if any influence on the cellular response and as such indicative of the fact that the coatings have no cytotoxicity to the cells. We further show that the cells attach well and spread actively on the coating surface with some cytoplasmic extensions, typical of the fibroblastic cellular growth (Fig. 8a and b). This is consistent with other

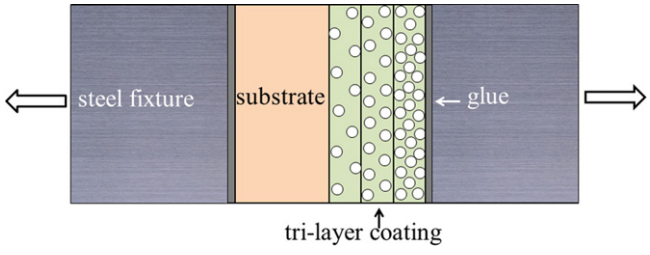

Fig. 6. Sketch of coating/substrate bonding strength test.

reports in the literature [49] which show a good in vitro cellular response on calcium phosphate surfaces.

The results of this work suggest that the layered calcium phosphate and zirconia based composite provides a potential promising alternative for large scale and load-bearing bone implant materials. However, the porosity, interconnectivity and pore size in the scaffold-like coating needs to be further enhanced for cell migration and for cell-cell communication throughout the entire scaffold structure so that osseointegration and bone regeneration can be realized. Further analysis of the scaffold inclusive of Fourier Transform Infrared Spectroscopy (FTIR), TEM-SAED/EDX and EDX dot

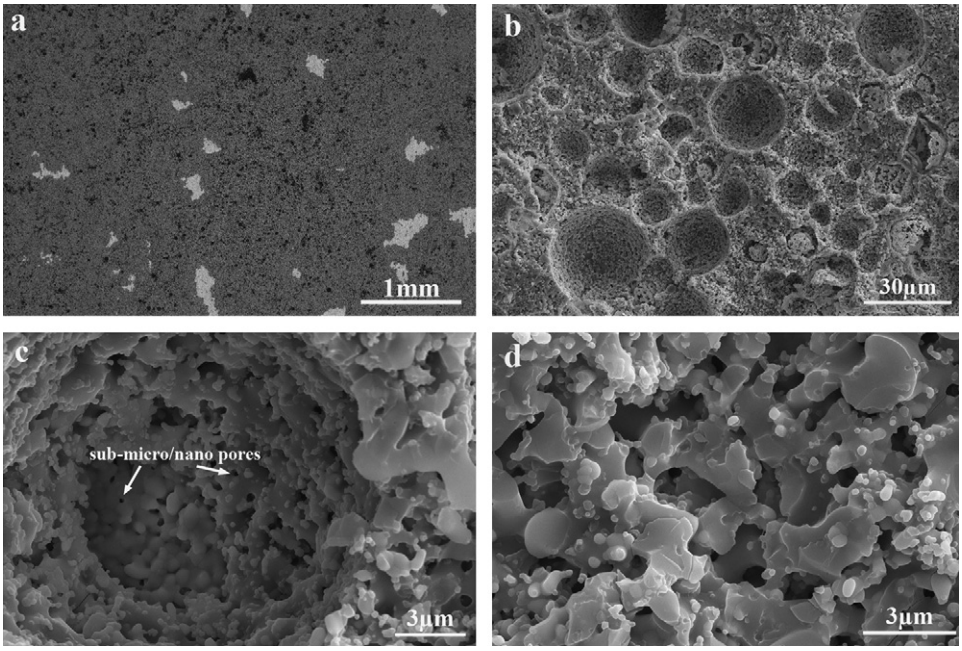

Fig. 7. Morphology of fracture surface of the transitional coating on zirconia based substrate after bonding strength test: (a) overview; (b) detailed porous structure; (c) and (d) close-ups of the round pore and connecting part with micro-sieve-like structure.

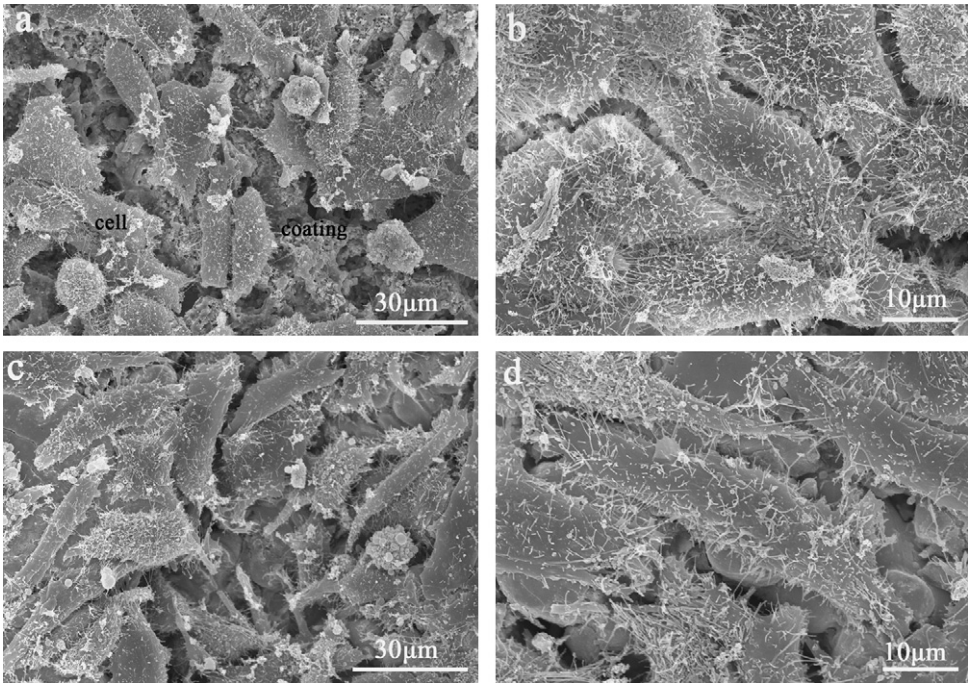

Fig. 8. SEM images showing the morphologies of cells proliferated onto the TCP-rich coatings and negative control material: (a) overview and (b) close-up of cells on top coating surface; (c) overview and (d) close-up of cells on bio-medical titanium alloy surface.

mapping/SEM-EPMA combined is required to determine precisely how the compositions and porous structures of calcium phosphate based coatings influence the biological and mechanical behavior of such composites.

5. Conclusions

In this paper we have designed a new layered bio-ceramic composite consisting of graded porous calcium phosphate coatings on strong load-bearing zirconia based substrate. These bio-functional-coating/strong-core composite have been manufactured using a slip coating-deposition and coating-substrate co-sintering technique. The resulting 200 μm thick coating has a hierarchical porous structure with nano/submicro pores and micro pores, and the cells can proliferate well on the non-cytotoxic calcium phosphate coating. The coating-substrate composite exhibits a very good bending strength and strong interfacial bonding. This porous bio-coating/strong-substrate composite provides a potential promising alternative for large scale and load-bearing bone implant replacement application.

Acknowledgments

This research was supported under the Australian Research Council's Discovery Projects funding scheme (project number DP110105296). The authors (JZY) and (RS) also respectively thank the China Scholarship Council and the Australian Postgraduate Research Award committee. The Gledden Senior Visiting Fellowship (ZHH) provided by the University of Western Australia is also greatly appreciated. We thank Prof. Yangai Liu for helping to do in vitro tests. The authors would like to thank the UWA Centre for Microscopy, Characterization and Analysis for the technical assistance to SEM study.

References

[1] M.A.K. Liebschner, M.A. Wettergreen, Optimization of Bone Scaffold Engineering for Load Bearing Applications, in: N. Ashammakhi, P. Ferretti (Eds.), Topics in Tissue Engineering, University of Oulu, Oulu, 2003, pp. 1–39.

[2] A.-M. Le Ray, H. Gautier, J.-M. Bouler, P. Weiss, C. Merle, A new technological procedure using sucrose as porogen compound to manufacture porous biphasic calcium phosphate ceramics of appropriate micro- and macrostructure, Ceramics International 36 (2010) 93–101.

[3] O. Gauthier, J.M. Bouler, E. Aguado, P. Pilet, G. Daculsi, Macroporous biphasic calcium phosphate ceramics: influence of macropore diameter and macroporosity percentage on bone ingrowth, Biomaterials 19 (1998) 133–139.

[4] A. Bignon, J. Chouteau, J. Chevalier, G. Fantozzi, J.P. Carret, P. Chavassieux, G. Boivin, M. Melin, D. Hartmannet, Effect of micro- and macroporosity of bone substitutes on their mechanical properties and cellular response, Journal of Materials Science: Materials in Medicine 14 (2003) 1089–1097.

[5] K.A. Hing, B. Annaz, S. Saeed, P.A. Revell, T. Buckland, Microporosity enhances bioactivity of synthetic bone graft substitutes, Journal of Materials Science: Materials in Medicine 16 (2005) 467–475.

[6] A. Macchetta, I.G. Turner, C.R. Bowen, Fabrication of HA/TCP scaffolds with a graded and porous structure using a camphene-based freeze-casting method, Acta Biomaterialia 5 (2009) 1319–1327.

[7] I.I.I.J. Cesarano, J.G. Dellinger, M.P. Saavedra, D.D. Gill, R.D. Jamison, B.A. Grosser, J.M. Sinn-Hanlon, M.S. Goldwasser, Customization of load-bearing ydroxyapatite lattice Scaffolds, International Journal of Applied Ceramic Technology 2 (2005) 212–220.

[8] Y. Zhang, D. Kong, Y. Yokogawa, X. Feng, Y.-Q. Tao, T. Qiu, Fabrication of porous hydroxyapatite ceramic scaffolds with high flexural strength through the double slip-casting method using fine powders, Journal of the American Ceramic Society 95 (2012) 147–152.

[9] J.D. Currey, What determines the bending strength of compact bone?, Journal of Experimental Biology 202 (1999) 2495–2503

[10] J.-R. Vignes, O. Jeelani, M. Dautheribes, F. San-Galli, D. Liguoro, Cranioplasty for repair of a large bone defect in a growing skull fracture in children, Journal of Cranio-Maxillofacial Surgery 35 (2007) 185–188.

[11] B. Elephterios, N. Dobrin, A. Chiriac, Titanium mesh cranioplasty for patients with large cranial defects - technical notes, Romanian Neurosurgery 17 (2010) 456–460.

[12] Eric Swarts, Alan Kop, Implant technology and biomaterials bulletin, Royal Perth Hospital 4 (2005) 1–5.

[13] D.-M. Liu, Q.Z. Yang, T. Troczynski, Sol–gel hydroxyapatite coatings on stainless steel substrates, Biomaterials 23 (2002) 691–698.

[14] H.-W. Kim, H.-E. Kim, J.C. Knowles, Hard-tissue-engineered zirconia porous scaffolds with hydroxyapatite sol–gel and slurry coatings, Journal of Biomedical Materials Research Part B: Applied Biomaterials 70B[2] (2004) 270–277.

[15] B.-Y. Chou, E. Chang, Interface investigation of plasma-sprayed hydroxyapatite coating on titanium alloy with ZrO_2 intermediate layer as bond coat, Scripta Materialia 45 (2001) 487–493.

[16] K.A. Khor, Y.W. Gu, C.H. Quek, P. Cheang, Plasma spraying of functionally graded hydroxyapatitey/Ti–6Al–4V coatings, Surface and Coating Technology 168 (2003) 195–201.

[17] Trevor Jones, Alan Kop, Eric Swarts, Rob Day, David Morrison, Susan Miller, Cathie Keogh, Implant technology and biomaterials bulletin, Royal Perth Hospital (2010) 1–4.

[18] J.-Z. Yang, R. Sultana, X.Z. Hu, Z.H. Huang, Porous hydroxyapatite coating on strong ceramic substrate fabricated by low density slip coating-deposition and coating-substrate co-sintering, Journal of European Ceramic Society 31 (2011) 2065–2071.

[19] L. Che, M. Gotoh, L. Yang, Y. Hirose, Residual stress state of hydroxyapatite graded coating on ceramic substrate, Advances in X-ray Analysis (2007))150–155.

[20] Z.Q. Wang, D.F. Xue, X.X. Chen, B.L. Lü, H. Ratajczak, Mechanical and biomedical properties of hydroxyapatite-based gradient coating on α-Al_2O_3 ceramic substrate, Journal of Non-Crystalline Solids 351 (2005) 1675–1681.

[21] Z.C. Wang, Y.J. Ni, J.C. Huang, Fabrication and characterization of HAp/Al_2O_3 composite coating on titanium substrate, Journal of Biomedical Science and Engineering 1 (2008) 190–194.

[22] R. Sultana, J.Z. Yang, X.Z. Hu, Processing of layered hydroxyapatite ceramic composites, Advanced Materials Research 275 (2011) 143–146.

[23] ASTM C1161-02c. Standard Test Method for Flexural Strength of Advanced Ceramics at Ambient Temperature.

[24] T. Mosmann, Rapid colorimetric assay for cellular growth and survival: application to proliferation and cytotoxicity assays, Journal of Immunological Methods 65 (1983) 55–63.

[25] D.S. Heo, J.G. Park, K. Hata, R. Day, R.B. Herberman, T.L. Whiteside, Evaluation of tetrazolium-based semiautomatic colorimetric assay for measurement of human antitumor cytotoxicity, Cancer Research 50 (1990) 3681–3690.

[26] S. Fujibayashi, M. Neo, H.-M. Kim, T. Kokubo, T. Nakamura, Osteoinduction of porous bioactive titanium metal, Biomaterials 25 (2004) 443–450.

[27] M. Takemoto, S. Fujibayashi, M. Neo, J. Suzuki, T. Kokubo, T. Nakamura, Mechanical properties and osteoconductivity of porous bioactive titanium, Biomaterials 26 (2005) 6014–6023.

[28] L.F. Cooper, A role for surface topography in creating and maintaining bone at titanium endosseous implants, Journal of Prosthetic Dentistry 84 (2000) 522–534.
[29] J.E. Nevelos, E. Ingham, C. Doyle, J. Fisher, A.B. Nevelos, Analysis of retrieved alumina ceramic components from Mittelmeier total hip prostheses, Biomaterials 20 (1999) 1833–1840.
[30] A.H. De Aza, J. Chevalier, G. Fantozzi, M. Schehl, R. Torrecillas, Crack growth resistance of alumina, zirconia andzirconia toughened alumina ceramics for joint prostheses, Biomaterials 23 (2002) 937–945.
[31] M.A. Germain, A. Hatton, S. Williams, J.B. Matthews, M.H. Stone, J. Fisher, E. Ingham, Comparison of the cytotoxicity of clinically relevant cobalt–chromium and alumina ceramic wear particles in vitro, Biomaterials 24 (2003) 469–479.
[32] G. Muralithran, S. Ramesh, The effects of sintering temperature on the properties of hydroxyapatite, Ceramics International 26 (2000) 221–230.
[33] Chun-Jen Liao, Feng-Huei Lin, Ko-Shao Chen, Jui-Sheng Sun, Thermal decomposition and reconstitution of hydroxyapatite in air atmosphere, Biomaterials 20 (1999) 1807–1813.
[34] T.F. Lang, A.D. Leblanc, H.J. Evans, Y. Lu, Adaptation of the proximal femur to skeletal reloading after long-duration spaceflight, Journal of Bone and Mineral Research 21 (2006) 1224–1230.
[35] T.M.G. Chu, S.J. Warden, C.H. Turner, R.L. Stewart, Segmental bone regeneration using a load-bearing biodegradable carrier of bone morphogenetic protein-2, Biomaterials 28 (2007) 459–467.
[36] S.J. Hollister, C.Y. Lin, E. Saito, R.D. Schek, J.M. Taboas, Engineering craniofacial scaffolds, Orthodontics and Craniofacial Research 8 (2005) 162–173.
[37] L. Rasmusson, K.-E. Kahnberg, A. Tan, Effects of implant design and surface on bone regeneration and implant stability: An experimental study in the dog mandible, Clinical Implant Dentistry and Related Research 3 (2001) 2–8.
[38] W. Suchanek, M. Yoshimura, Processing and properties of hydroxyapatite based biomaterials for use as hard tissue replacement implants, Journal of Materials Research 13 (1998) 94–114.
[39] C. Schopper, F. Ziya-Ghazvini, W. Goriwoda, D. Moser, F. Wanschitz, E. Spassova, G. Lagogiannis, A. Auterith, R. Ewers, HA/TCP compounding of a porous cap biomaterial improves bone formation and scaffold degradation-A long-term histological study, Wiley InterScience (www.interscience.wiley.com). http://dx.doi.org/10.1002/jbm.b.30199.
[40] H.H.K. Xu, E.F. Burguera, L.E. Carey, Strong, macroporous, and in situ-setting calcium phosphate cement-layered structures, Biomaterials 28 (2007) 3786–3796.
[41] H.H.K. Xu, M.D. Weir, E.F. Burguera, A.M. Fraser, Injectable and macroporous calcium phosphate cement scaffold, Biomaterials 27 (2006) 4279–4287.
[42] J.R. Woodard, A.J. Hilldore, S.K. Lan, C.J. Park, A.W. Morgan, J.A.C. Eurell, S.G. Clark, M.B. Wheeler, R.D. Jamison, A.J.W. Johnson, The mechanical properties and osteoconductivity of hydroxyapatite bone scaffolds with multi-scale porosity, Biomaterials 28 (2007) 45–54.
[43] A. Slosarczyk, Highly porous hydroxyapatite material, Powder Metallurgy International 21 (1989) 24–25.
[44] E. Fidancevska, G. Ruseska, J. Bossert, Y.-M. Lin, A.R. Boccaccini, Fabrication and characterization of porous bioceramic composites based on hydroxyapatite and titania, Materials Chemistry and Physics 103 (2007) 95–100.
[45] B.V. Krishna, S. Bose, A. Bandyopadhyay, Low stiffness porous Ti structures for load-bearing implants, Acta Biomaterialia 3 (2007) 997–1006.
[46] Y.-S. Chang, M. Oka, M. Kobayashi, H.-O. Gu, Z.-L. Li, T. Nakamura, Y. Ikada, Significance of interstitial bone ingrowth under load-bearing conditions: a comparison between solid and porous implant materials, Biomaterials 17 (1996) 1141–1148.
[47] G.-B. Wei, P.X. Ma, Nanostructured biomaterials for regeneration, Adv. Funct. Mater. 18 (2008) 3568–3582.
[48] A.M. Lipski, C. Jaquiery, H. Choi, D. Eberli, M. Stevens, I. Martin, I.W. Chen, V.P. Shastri, Nanoscale Engineering of Biomaterial Surfaces, Advanced Materialia 19 (2007) 553–557.
[49] Sahil Jalota, B. Bhaduri, A. Cuneyt Tas, Osteoblast proliferation on neat and apatite-like calcium phosphate-coated titanium foam scaffolds, Materials Science and Engineering C 27 (2007) 432–440.